Supplementary Materials for

Capillary Skimming Floating Microplastics via a Water-Bridged Ratchet

Seohyun Cho, Sang Jin Park, Young Jin Lee, You Jun Lee, Young A Lee, Ho-Young Kim, Seong Jin Kim*, Seok Chung and Myoung-Woon Moon*

*Corresponding author. Email: kyk756@kist.re.kr (S. J. K.); mwmoon@kist.re.kr (M.-W. M.)

This PDF file includes:

Supplementary Text
Figs. S1 to S10
Tables S1 to S2
Legends for movies S1 to S9
References (34, 51 to 66)

Other Supplementary Materials for this manuscript include the following:

Movie S1 (.mp4 format). Collecting the various MPs using the hydrophilic ratchet drum.
Movie S2 (.mp4 format). EPS foam ball being skimmed by the hydrophilic ratchet plate.
Movie S3 (.mp4 format). Skimming small and large EPS foam balls using a hydrophilic flat plate.
Movie S4 (.mp4 format). Flow vector field generated while lifting the ratchet plate.
Movie S5 (.mp4 format). Flow vector field generated while lifting the flat plate.
Movie S6 (.mp4 format). Capillary water bridge ruptured and skimming failed.
Movie S7 (.mp4 format). The ratchet plate failed to skim a single PE pellet (P = H = 6 mm).
Movie S8 (.mp4 format). Tilting the ratchet plate at + 30° to skim a single PE pellet (P = H = 6 mm).
Movie S9 (.mp4 format). Skimming and release behavior of PP on the hydrophilic ratchet drum.

Supplementary Text

Capillary skimming with Cheerios effect.

A solid object floating on water experiences the directional force from the surrounding curved capillary water meniscus (*34, 51−53*). This phenomenon has been studied in the context of water-walking insects, such as the larva of the waterlily leaf beetle Pyrrhalta, which climb on water meniscus by adjusting their body shape to take advantage of the directional force generated by the curved water meniscus (*54*). The phenomenon of directional force between two solid objects, which is generated by a curved liquid meniscus, is commonly referred to as the "Cheerios effect". This term originates from the behavior of Cheerios breakfast cereal floating in milk, which tend to clump together or adhere to the walls of the container. (*34*). The Cheerios effect has been used to explain a range of natural phenomena, such as the clustering of aquatic plants in certain areas due to the adherence of floating seeds to one another and to other plants or rocks (*55, 56*). It was observed that MPs floating on the water also exhibit interactions with one another and with surrounding object. The direction of the force is determined by the shape of the water meniscus formed between the two objects. Figure S9 shows the direction of the force depending on the shape of the water meniscus. When the menisci between the plate and the ball are formed by combining concave and concave shapes (magenta contour in fig. S9A), or convex and convex shapes (blue contour in fig. S9B), attractive force is generated. Conversely, when the menisci are formed by combining concave and convex shapes (fig. S9C), or convex and concave shapes (fig. S9D), the plate and the ball experience repulsion force. When the plate is tilted in the negative (−) direction, the height of the concave water meniscus increases, resulting in an increase in the magnitude of the repulsion force generated (fig. S9E). When the plate is tilted in the positive (+) direction, the height of the concave water meniscus decreases (red contour in fig. S9F), resulting in the disappearance of the repulsion force. In this way, the MP floating on water can receive directional force in various ways depending on the buoyancy of the MP and the angle of inclination of the plate (*51, 52, 57−59*).

The buoyancy of MPs could vary due to the wide range of shapes, densities, and sizes. The EPS foam balls and PE pellets were shown floating in water in a glass container (fig. S10A) and a PS container (fig. S10B), respectively. On the hydrophilic glass container wall, a concave water meniscus was formed, and the EPS foam ball was observed to form the concave water meniscus and contact the container due to the attraction force. Furthermore, EPS foam balls were observed to float at a distance from PE pellets, which formed convex water meniscus in their vicinity. As shown in Figure S10B, the formation of convex meniscus on the hydrophobic PS container wall indicated that the PE pellets were in contact with the container wall. We have confirmed that MPs, which form concave water meniscus in their vicinity, such as EPS foam balls, can assist in capillary skimming by providing attraction force when utilizing hydrophilic surface. MPs with density similar to that of water, such as PE and PP pellets, were found to experience a repulsive force near the concave water meniscus formed on the hydrophilic surface, resulting in no contact with the plate surface. Even on a hydrophilic surface, tilting in the + direction resulted in the formed concave water meniscus being almost identical to the free surface of water, thereby eliminating the repulsion force generated by the Cheerios effect (Fig. 7B in the main text). Eventually, the PE pellets were capillary skimmed by tilting the ratchet plate (Fig. 7D in the main text).

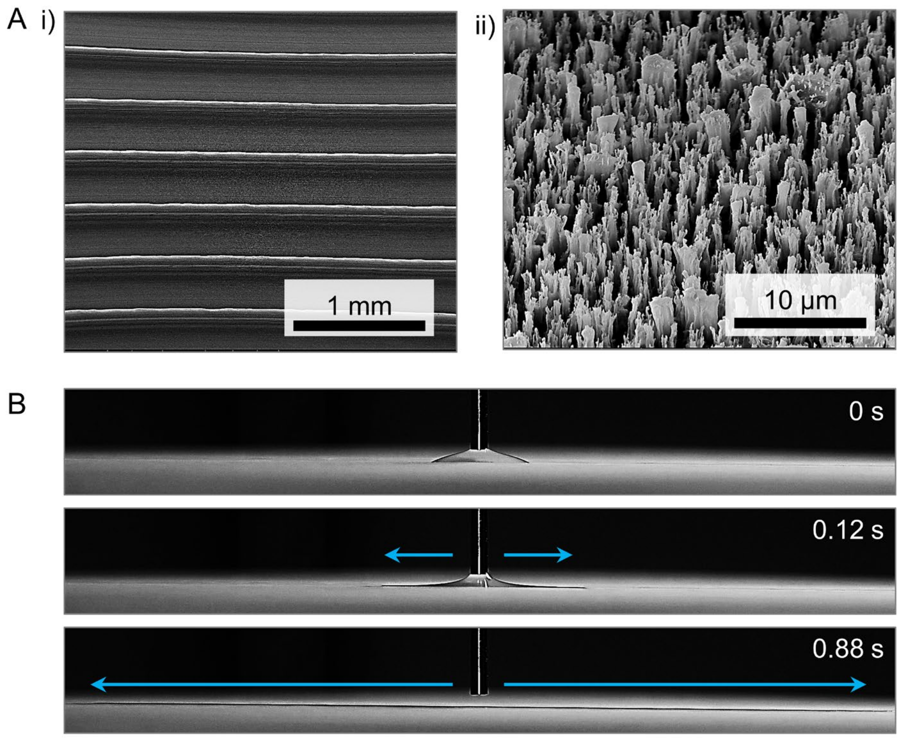

Fig. S1. Surface characteristics of oxygen plasma treated Polylactic Acid (PLA). (**A**) SEM images of the oxygen plasma treated surface of PLA. (i) 100X, showing the rastered line pattern by a 3D printer and (ii) 10,000X, showing a high-aspect-ration nanostructures formed by oxygen plasma etching. (**B**) Optical images showing the sequential behavior of the water spreading behavior on the hydrophilic PLA surface.

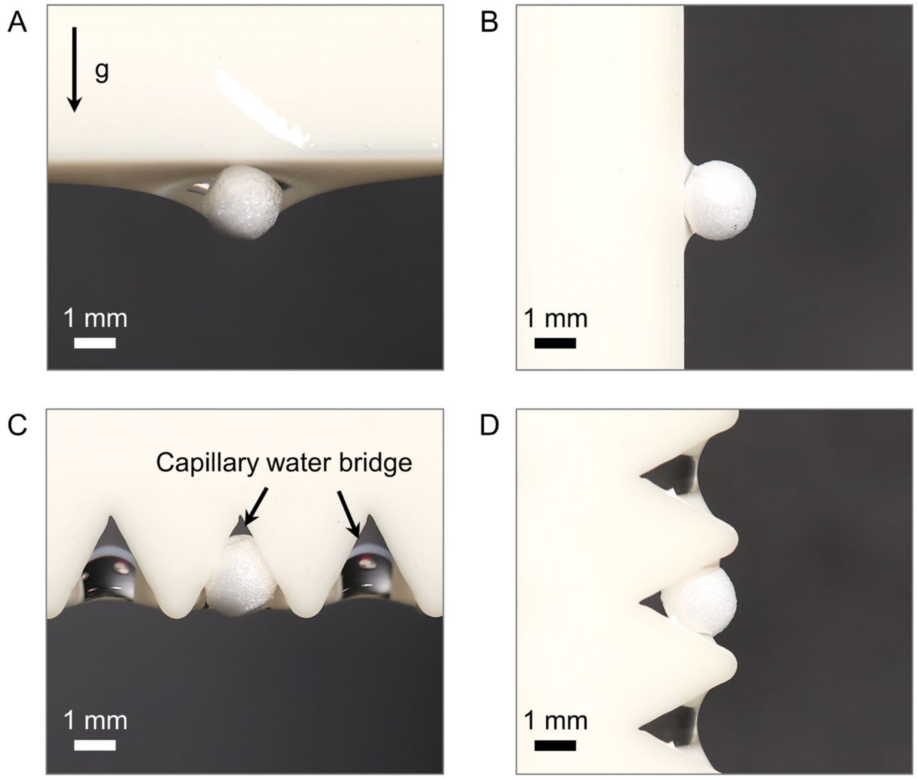

Fig. S2. Formation of a stable capillary adhesion with a water bridge. Optical images showing EPS foam balls held on (**A**) the flat plate normal to gravity and (**B**) the flat plate parallel to gravity. Optical images showing the EPS foam ball held on (**C**) the ratchet plate normal to gravity and (**D**) the ratchet plate parallel to gravity. Arrows indicate the capillary water bridge formed between the ratchet tooth.

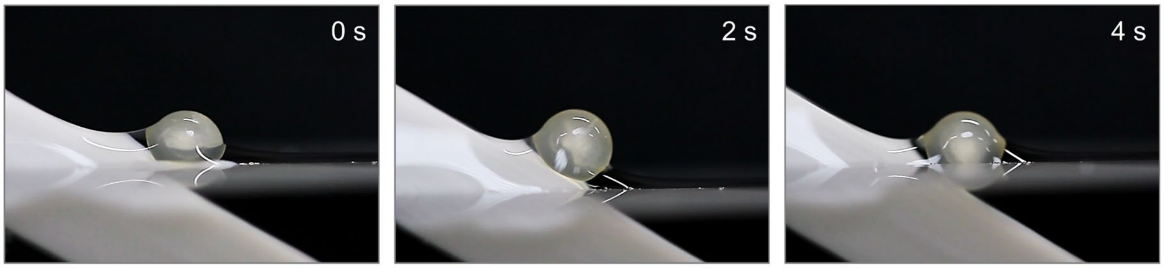

Fig. S3. Sequential images of failed attempts to skim a 3-mm polypropylene (PP) ball using a flat plate tilted at + 60°. For the initial 2s, the PP ball adhered to the plate and lifted before sliding down as the upper water bridge receded (4 s).

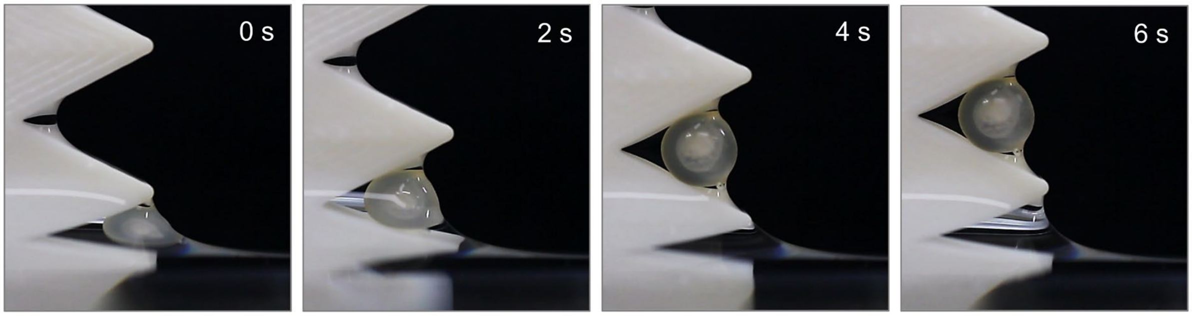

Fig. S4. Sequential images of capillary skimming a 3-mm polypropylene (PP) ball using a ratchet structure. The water bridge formed around the PP ball, maintaining stable capillary adhesion.

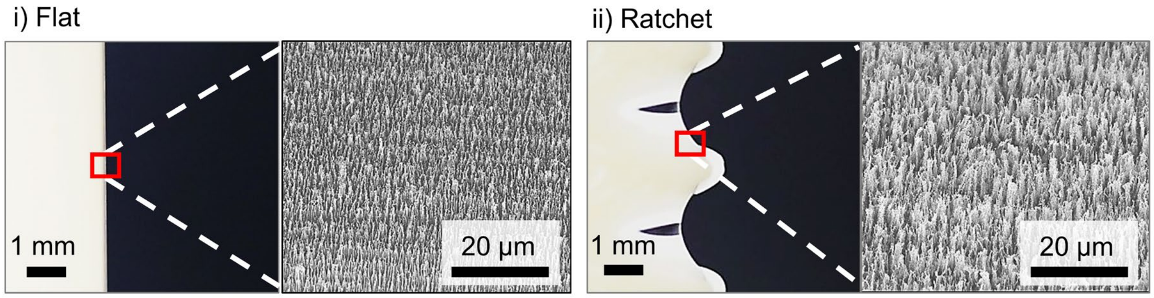

Fig. S5. Surface characteristics of Polylactic acid (PLA) with ratchet structure. An optical image of the plate and a SEM image of the indicated area captured at a higher magnification (5,000X), i) the flat plate, ii) the ratchet plate in the side view. All surfaces are hydrophilic, with the ratchet in particular being capable of containing a significant amount of water internally.

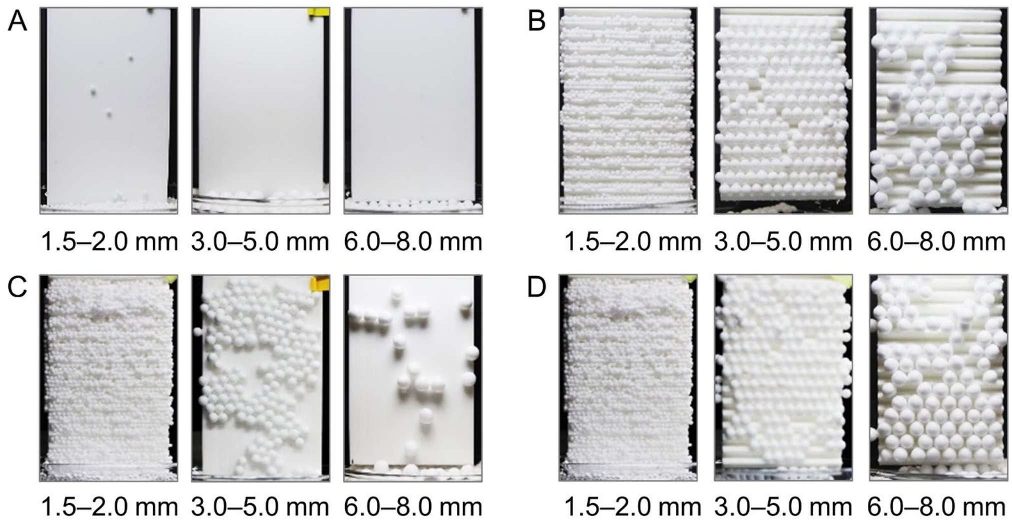

Fig. S6. Optical images of EPS foam balls skimmed on the four different plates with three different sets of the ball diameters (1.5−2.0, 3.0−5.0 and 6.0−8.0 mm in diameter). Optical mages in the front view showing the 4 different types of the skimming surfaces; (**A**) the hydrophobic flat, (**B**) the hydrophobic ratchet, (**C**) the hydrophilic flat, (**D**) the hydrophilic ratchet.

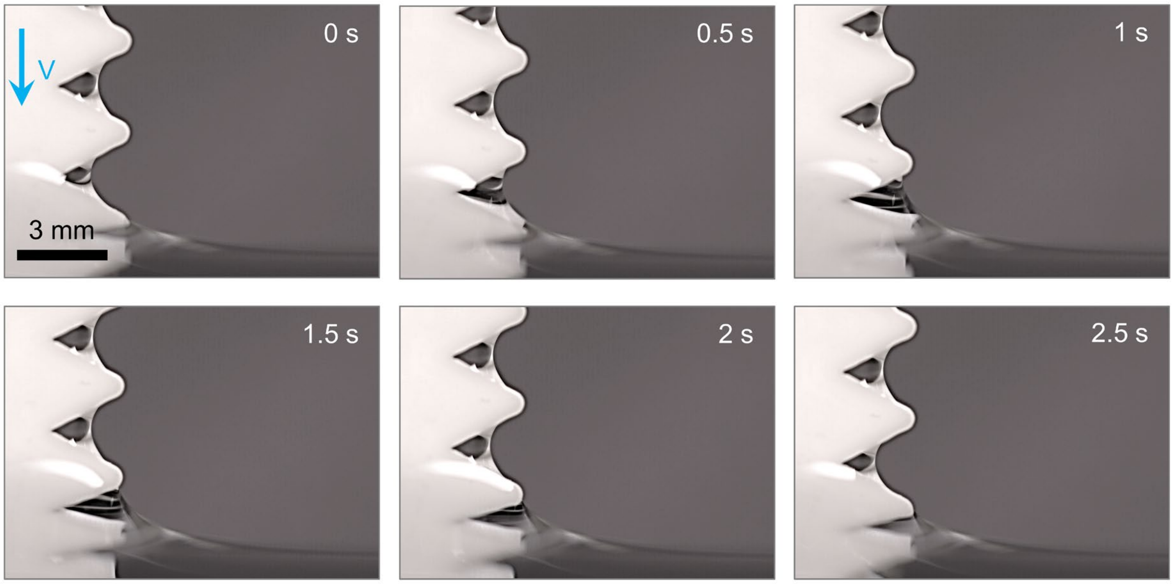

Fig. S7. Optical images of the meniscus evolution sequentially upon dipping the ratchet plate in water in the side view. When the water contained inside the ratchet came into contact with the external water, the meniscus thickened and transformed into an outwardly curved shape with time.

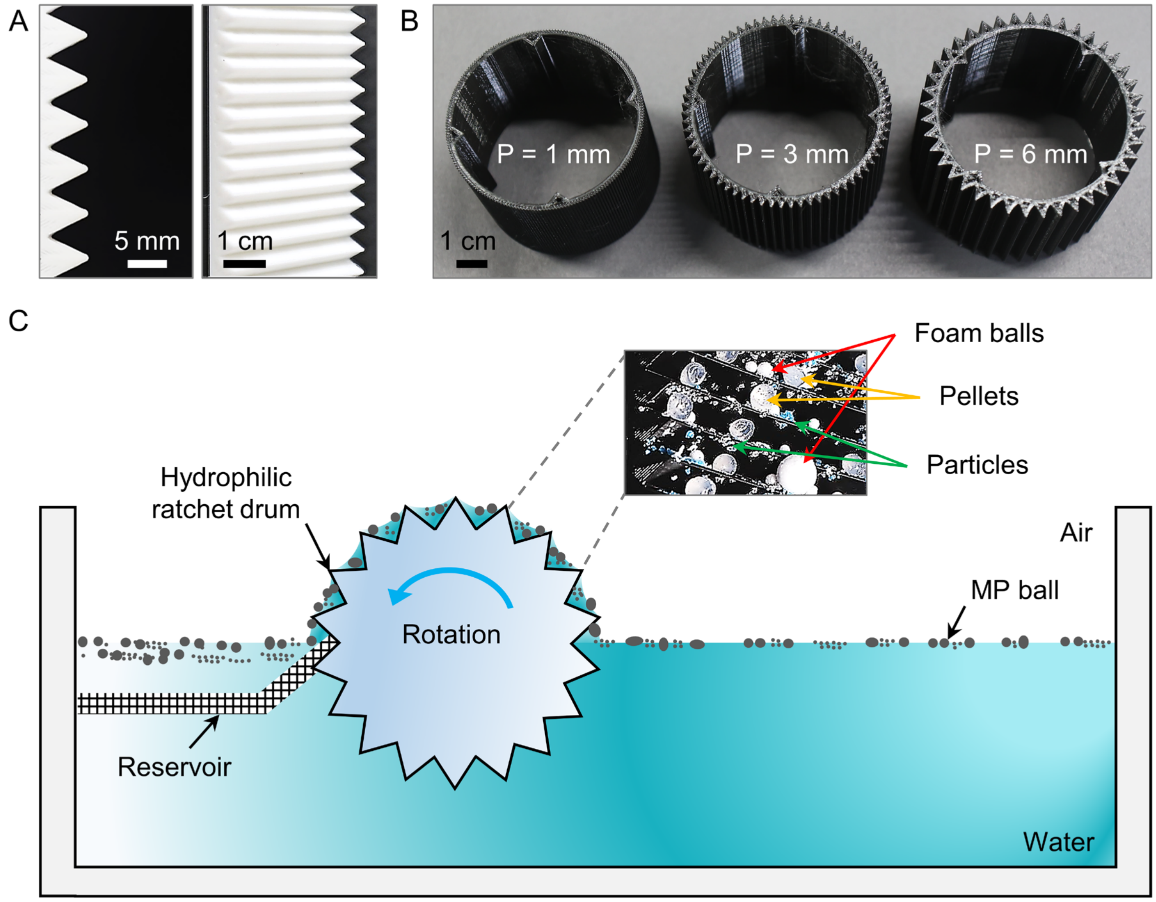

Fig. S8. 3D-printed ratchet structures in various shapes and a setup for direct MP recovery with the ratchet drum system. Optical images showing (**A**) the plate-type ratchet and (**B**) the drum-type ratchet. (**C**) A schematic for the experimental set-up collecting the microplastics by the drum-type ratchet structure. MPs are skimmed from the right side of the ratchet drum and released into the left side, at which the released MPs are collected within the reservoir. An inset image showing the ratchet surface having several types of MP particles such as EPS foam balls, PP pellets, PP particles, PE pellets and PE particles in various size and density (see the data for the density and shape in **Table S2**).

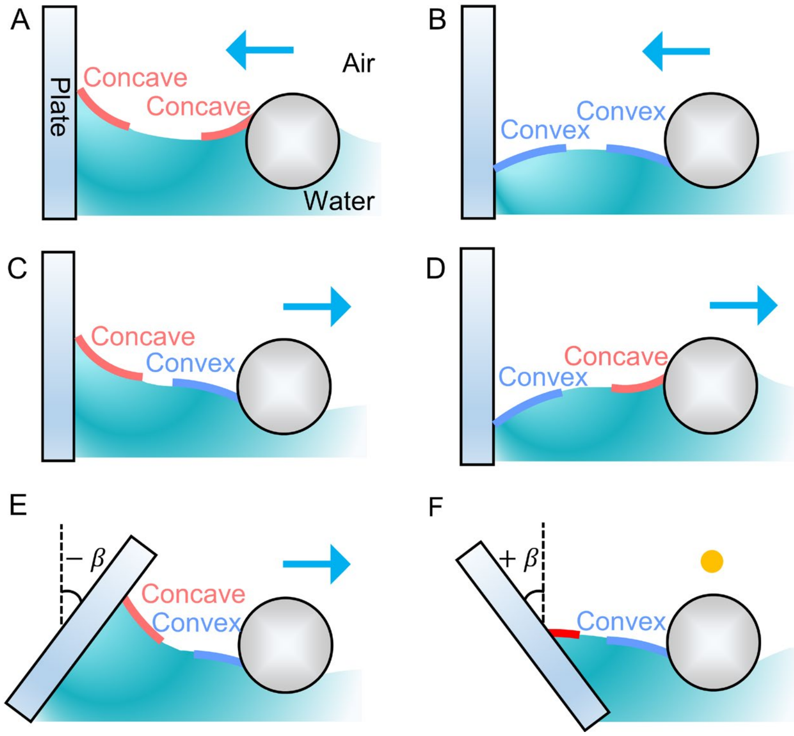

Fig. S9. Schematics of the meniscus formation on the plate and MPs, and the resulting directional force direction. When the menisci between the plate and the ball are formed by combining concave and concave shapes (magenta contour) in (**A**), or convex and convex shapes (blue contour) in (**B**), attractive force is generated. Conversely, when the menisci are formed by combining concave and convex shapes (**C**), or convex and concave shapes (**D**), the plate and the ball experience repulsion force. (**E**) When the plate is tilted in the − direction, the height of the concave water meniscus increases, resulting in an increase in the magnitude of the repulsion force generated. (**F**) When the plate is tilted in the + direction, the height of the concave water meniscus decreases (red contour), resulting in the disappearance of the repulsion force.

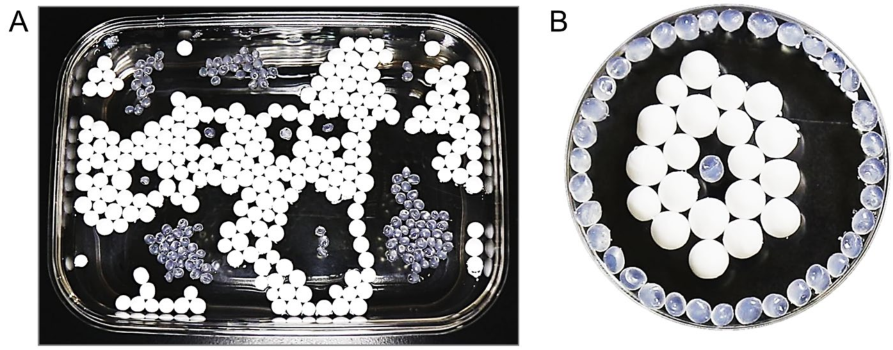

Fig. S10. **Top-down view of an optical image capturing EPS foam balls and PE pellets floating on the water.** Cheerios phenomena with EPS foam balls (white) and PE pellets (translucent) contained in a water-filled hydrophilic glass container (**A**) and a hydrophobic PS container (**B**).

Ball Name	Material	Diameter (mm)	Infill density (%)	Mass (mg)	Density (g cm^{-3})
ED1	EPS foam	2	-	0.15 ± 0.02	0.04 ± 0.005
ED2		6	-	2.6 ± 0.2	0.02 ± 0.005
ED3		10	-	12 ± 0.2	0.02 ± 0.005
ED4		15	-	29 ± 0.5	0.02 ± 0.005
ED5		20	-	73 ± 0.5	0.02 ± 0.005
ED6		30	-	225 ± 0.5	0.02 ± 0.005
PD1I0	Polylactic Acid (3-D printed PLA)	6	0	85 ± 0.5	0.75 ± 0.02
PD1I25			25	88 ± 0.5	0.78 ± 0.02
PD1I50			50	93 ± 0.5	0.82 ± 0.02
PD2I0		9	0	224 ± 0.5	0.59 ± 0.02
PD2I25			25	235 ± 0.5	0.61 ± 0.02
PD2I50			50	299 ± 0.5	0.78 ± 0.02
PD3I0		12	0	400 ± 0.5	0.44 ± 0.02
PD3I25			25	469 ± 0.5	0.52 ± 0.02
PD3I50			50	625 ± 0.5	0.69 ± 0.02

Table. S1. The properties of the ball used in the skimming experiment. The table shows the diameter, mass, and density of 3D printed PLA balls and EPS foam balls. The density of 3D printed PLA balls varied depending on the infill density. ED represents EPS diameter in order, PD represents PLA diameter in order, and I represents infill density.

Plastic	Chemical formula	Density (g cm^{-3})	Contact angle (°)	Shape	
PS	$(C_8H_8)_n$	Foam : 0.02 – 0.04 (1.04 – 1.5) [44, 60]	88 – 92 [61]	Foam	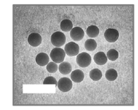
PE	$(C_2H_4)_n$	0.92 – 0.97 [44, 60]	100 – 103[62–64]	Pellet	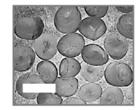
				Particle	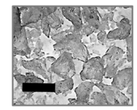
PP	$(C_3H_6)_n$	0.88 – 0.91 [44]	99.8 – 111.5 [65, 66]	Pellet	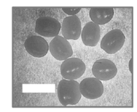
				Particle	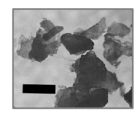

Table. S2. **Material properties of the plastic commonly found floating in the ocean.** The types and conditions of plastics were classified into five categories. The table shows the chemical formula, density, contact angle and shape (*44, 60−66*). The white scale bar is 5 mm, the black scale bar is 0.5 mm.

Supplementary Movie Legends

Movie S1. Collecting the various MPs using the hydrophilic ratchet drum. A movie clip shows the recovery of the various MPs floating on water. The ratchet drum recovered EPS foam balls, PP pellets, PP particles, PE pellets, and PE particles (played at 1x speed).

Movie S2. EPS foam ball being skimmed by the hydrophilic ratchet plate. A movie clip shows a series of processes where EPS foam ball was skimmed and released using a ratchet plate. (played at 1x speed).

Movie S3. Skimming small and large EPS foam balls using a hydrophilic flat plate. A movie clip shows the skimming of EPS foam balls with diameters of 2 mm and 5 mm at a lifting speed of 1 mm/s using a hydrophilic flat plate. (played at 1x speed).

Movie S4. Flow vector field generated while lifting the ratchet plate. A movie clip shows the flow vector field generated by the lifting of the ratchet plate at a speed of 50 mm/s (played at 1/75x speed).

Movie S5. Flow vector field generated while lifting the flat plate. A movie clip shows the flow vector field generated by the lifting of the flat plate at a speed of 50 mm/s (played at 1/75x speed).

Movie S6. Capillary water bridge ruptured and skimming failed. A movie clip shows that when the size of the ratchet and the ball became too large, the capillary water bridge inside the ratchet ruptured and skimming failed (played at 1x speed).

Movie S7. The ratchet plate failed to skim a single PE pellet (P = H = 6 mm). A movie clip shows the failure to skim a single PE pellet (played at 1x speed).

Movie S8. Tilting the ratchet plate at + 30° to skim a single PE pellet (P = H = 6 mm). A movie clip shows the tilted ratchet plate skimming a single PE pellet (played at 1x speed).

Movie S9. Skimming and release behavior of PP on the hydrophilic ratchet drum. A movie clip shows the skim and release behavior of the MPs floating on water. It exhibited a skimming behavior for the first 4-5 seconds, followed by a releasing behavior (played at 1x speed).

RERENCES AND NOTES

1. E. J. Carpenter, S. J. Anderson, G. R. Harvey, H. P. Miklas, B. B. Peck, Polystyrene spherules in coastal waters. *Science* **178**, 749-750 (1972).
2. R. C. Thompson, Y. Olsen, R. P. Mitchell, A. Davis, S. J. Rowland, A. W. G. John, D. Mcgonigle, A. E. Russell, Lost at Sea: Where Is All the Plastic? *Science* **304**, 838 (2004).
3. J. A. Ivar Do Sul, M. F. Costa, The present and future of microplastic pollution in the marine environment. *Environ. Pollut.* **185**, 352-364 (2014).
4. W. Perren, A. Wojtasik, Q. Cai, Removal of Microbeads from Wastewater Using Electrocoagulation. *ACS Omega* **3**, 3357-3364 (2018).
5. C. Wang, J. Zhao, B. Xing, Environmental source, fate, and toxicity of microplastics. *J. Hazard. Mater.* **407**, 124357 (2021).
6. H. Yang, G. Chen, J. Wang, Microplastics in the Marine Environment: Sources, Fates, Impacts and Microbial Degradation. *Toxics* **9**, 41 (2021)
7. M. E. Miller, F. J. Kroon, C. A. Motti, Recovering microplastics from marine samples: A review of current practices. *Mar. Pollut. Bull.* **123**, 6-18 (2017).
8. A. L. Andrady, Microplastics in the marine environment. *Mar. Pollut. Bull.* **62**, 1596-1605 (2011).
9. A. A. Koelmans, P. E. Redondo-Hasselerharm, N. H. Mohamed Nor, V. N. de Ruijter, S. M. Mintenig, Merel Kooi, Risk assessment o f microplastic particles. *Nat. Rev. Mater.* **7**, 138 (2022).
10. J. Gigault, H.E. Hadri, B. Nguyen, B. Grassl, L Rowenczyk, N. Tufenkji, S. Feng, M. Wiesner, Nanoplastics are neither microplastics nor engineered nanoparticles. *Nat. Nanotechnol.* **16**, 501-507 (2021).
11. A. Turner, Foamed Polystyrene in the Marine Environment: Sources, Additives, Transport, Behavior, and Impacts. *Environ. Sci. Tech nol.* **54**, 10411-10420 (2020).
12. L. Vuori, M. Ollikainen, How to remove microplastics in wastewater? A cost-effectiveness analysis. *Ecol. Econ.* **192**, 107246 (2022).
13. C. Li, R. Busquets, L. C. Campos, Assessment of microplastics in freshwater systems: A review. *Sci. Total Environ.* **707**, 135578 (202 0).
14. H. A. Leslie, M. J. M. van Velzen, S. H. Brandsma, A. D. Vethaak, J. J. Garcia-Vallejo, M. H. Lamoree, Discovery and quantification of plastic particle pollution in human blood. *Environ. Int.* **163**, 107199 (2022).
15. A. D. Vethaak, J. Legler, Microplastics and human health. *Science* **371**, 672-674 (2021).
16. A. A. Adelodun, Plastic Recovery and Utilization: From Ocean Pollution to Green Economy. *Front. Environ. Sci.* **9**, 683403 (2021).
17. J. Wang, X. Liu, Y. Li, T. Powell, X. Wang, G. Wang, P. Zhang, Microplastics as contaminants in the soil environment: A mini-revie w. *Sci. Total Environ.* **691**, 848-857 (2019).
18. S. L. Wright, R. C. Thompson, T. S. Galloway, The physical impacts of microplastics on marine organisms: A review, *Environ. Pollut.* **178**, *483-492* (2013).
19. C. Pedà, L. Caccamo, M. C. Fossi, F. Gai, F. Andaloro, L. Genovese, A. Perdichizzi, T. Romeo, G. Maricchiolo, Intestinal alterations i n European sea bass Dicentrarchus labrax (Linnaeus, 1758) exposed to microplastics: Preliminary results. *Environ. Pollut.* **212**, 251-25 6 (2016).
20. B. Nguyen, D. Claveau-Mallet, L. M. Hernandez, E. G. Xu, J. M. Farner, N. Tufenkji, Separation and Analysis of Microplastics and N anoplastics in Complex Environmental Samples. *Acc. Chem. Res.* **52**, 858-866 (2019).
21. J. C. Prata, J. P. da Costa, A. C. Duarte, T. Rocha-Santos, Methods for sampling and detection of microplastics in water and sediment: A critical review. *Trends Anal. Chem.* **110**, 150-159 (2019).
22. D. Kaiser, N. Kowalski, J. J. Waniek, Effects of biofouling on the sinking behavior of microplastics. *Environ. Res. Lett.* **12**, 124003 (2 017).
23. Y. Liu, B. Wang, V. Pileggi, S. Chang, Methods to recover and characterize microplastics in wastewater treatment plants. *Case Stud. C hem. Environ. Eng.* **5**, 100183 (2022).
24. W. Zhang, S. Zhang, J. Wang, Y. Wang, J. Mu, P. Wang, X. Lin, D. Ma, Microplastic pollution in the surface waters of the Bohai Sea, China. *Environ. Pollut.* **231**, 541-548 (2017).
25. K. Uchida, M. Kuroda, T. Tokai, Comparison of Microplastic Sampling Performance between a Neuston Net and a Manta Net. *Fisheri es Eng.* **59**, 19-26 (2022).
26. T. Montoto-Martínez, C. Meléndez-Díez, A. Melián-Ramírez, J. J. Hernández-Brito, M. D. Gelado-Caballero, Comparison between th e traditional Manta net and an innovative device for microplastic sampling in surface marine waters. *Mar. Pollut. Bull.* **185**, 144237 (2 022).
27. G. Pasquier, P. Doyen, M. Kazour, A. Dehaut, M. Diop, G. Duflos, R. Amara, Manta Net: The Golden Method for Sampling Surface Water Microplastics in Aquatic Environments. *Front. Environ. Sci.* **10**, 811112 (2022).
28. T. Wang, H. J. Joo, S. Song, W. Hu, C. Keplinger, M. Sitti, A versatile jellyfish-like robotic platform for effective underwater propulsi on and manipulation. *Sci. Adv*. **9**, eadg0292 (2023).
29. N. Bhardwaj, A. N. Bhaskarwar, A review on sorbent devices for oil-spill control. *Environ. Pollut.* **243**, 1758-1771 (2018).
30. A. T. Hoang, X. P. Nguyen, X. Q. Duong, T. T. Huynh, Sorbent-based devices for the removal of spilled oil from water: a review. *Env iron. Sci. Pollut. Res.* **28**, 28876-28910 (2021).
31. T. J. Ko, S. Cho, S. J. Kim, Y. A. Lee, D. H. Kim, W. Jo, H. Y. Kim, S. Yang, K. H. Oh, M. W. Moon, Direct recovery of spilled oil u sing hierarchically porous oil scoop with capillary-induced anti-oil-fouling. *J. Hazard. Mater.* **410**, 124549 (2021).
32. Y. A. Lee, Y. C. Park, O. Kwon, S. J. Kim, S. Chung, M. W. Moon, Hygroscopic Ramie Fabrics for Recovering Highly Viscous Low Sulfur Fuel Oil, *Environ. Pollut.* **308**, 119668 (2022).
33. Y. A. Lee, S. Cho, S. Choi, O. Kwon, S. M. Yoon, S. J. Kim, K. C. Park, S. Chung, M. W. Moon, Slippery, Water-Infused Membrane with Grooved Nanotrichomes for Lubricating-Induced Oil Repellency. *Adv. Sci.* **9**, 2103950 (2022).
34. D. Vella, L. Mahadevan, The "Cheerios effect". *Am. J. Phys.* **73**, 817 (2005).
35. I. Ho, G. Pucci, D. M. Harris, Direct Measurement of Capillary Attraction between Floating Disks. *Phys. Rev. Lett.* **123**, 254502 (201 9).
36. J. Meseguer, L. A. Slobozhanin, J. M. Perales, A REVIEW ON THE STABILITY OF LIQUID BRIDGES. *Adv. Space Res.* **16**, 7, 5-1 4 (1995).
37. S. Reddy, P. R. Schunk, R. T. Bonnecaze, Dynamics of low capillary number interfaces moving through sharp features. *Phys. Fluids.* **17**, 122104 (2005).

38. J. E. Seebergh, J. C. Berg, Dynamic wetting in the low capillary number regime. *Chem. Eng. Sci.* **47**, 4455-4464 (1992).
39. I. chatzis, N. R. Morrow, Correlation of Capillary Number Relationships for Sandstone. *Soc. Pet. Eng. J.* **24**, 555-562 (1984).
40. J. Park, C. Lee, S. Lee, H. Cho, M. W. Moon, S. J. Kim, Clogged water bridges for fog harvesting. *Soft Matter.* **17**, 136 (2021).
41. D. J. Broesch, J. Frechette, From Concave to Convex: Capillary Bridges in Slit Pore Geometry. *Langmuir* **28**, 15548-15554 (2012).
42. T. M. Karlsson, L. Arneborg, G. Broström, B. C. Almroth, L. Gipperth, M. Hassellöv, The unaccountability case of plastic pellet pollu tion. *Mar. Pollut. Bull.* **129**, 52-60 (2018).
43. M. Sewwandi, O. Hettithanthri, S. M. Egodage, A. A. D. Amarathunga, M. Vithanage, Unprecedented marine microplastic contaminat ion from the X-Press Pearl container vessel disaster. *Sci. Total Environ.* **828**, 154374 (2022).
44. A. Stubbins, K. L. Law, S. E. Muñoz, T. S. Bianchi, L. Zhu, Plastics in the Earth system. *Science* **373**, 51-55 (2021).
45. H. J. Butt, M. Kappl, Normal capillary forces. *Adv. Colloid Interface Sci.* **146**, 48-60 (2009).
46. B. Mielniczuk, T. Hueckel, M. S. El Youssoufi, Laplace pressure evolution and four instabilities in evaporating two-grain liquid bridg es. *Powder Technol.* **283**, 137-151 (2015).
47. S. Mishima, H. Iikura, T. Ougizawa, Study of adhesion between microspheres and rubber surfaces accompanied by meniscus formatio n and sedimentation. *Appl. Adhes. Sci.* **5**, 5 (2017).
48. Y. Hou, B. Xue, S. Guan, S. Feng, Z. Geng, X. Sui, J. Lu, L. Gao, L. Jiang, Temperature-controlled directional spreading of water on a surface with high hysteresis. *NPG Asia Mater.* **5**, e77 (2013).
49. S. Ouenzerfi, S. Harmand, Experimental Droplet Study of Inverted Marangoni Effect of a Binary Liquid Mixture on a Nonuniform He ated Substrate. *Langmuir* **32**, 2378-2388 (2016).
50. W. Thielicke, R. Sonntag, Particle Image Velocimetry for MATLAB: Accuracy and enhanced algorithms in PIVlab. *J. Open Res. Soft w.*, 9-12 (2021).
51. C. Zhao, L. Cai, M. Nie, L. Shang, Y.Wang, Y. Zhao, Cheerios Effect Inspired Microbubbles as Suspended and Adhered Oral Deliver y Systems. *Adv. Sci.* **8**, 2004184 (2021).
52. G. Xie, P. Li, P. Y. Kim, P. Y. Gu, B. A. Helms, P. D. Ashby, L. Jiang, T. P. Russell, Continuous, autonomous subsurface cargo shuttl ing by nature-inspired meniscus-climbing systems. *Nat. Chem.* **14**, 208-215 (2022).
53. J. Liu, S. Li, Capillarity-driven migration of small objects: A critical review. *European Physical Journal E* **42**, 1 (2019).
54. D. L. Hu, J. W. M. Bush, Meniscus-climbing insects. *Nature* **437**, 733-736 (2005).
55. P. Peruzzo, A. Defina, H. Nepf, Capillary trapping of buoyant particles within regions of emergent vegetation. *Water Resour. Res.* **48**, W07512 (2012).
56. X. Liu, Y. Zeng, W. Huai, Floating seed dispersal in open channel flow with emergent vegetation. *Ecohydrology* **12**, e2038 (2019).
57. K. Katoh, H. Fujita, E. Imazu, Motion of a particle floating on a liquid meniscus surface. *J. Fluids Eng. Trans. ASME.* **114**, 411 (1992).
58. P. A. Kralchevsky, K. Nagayama, "LATERAL CAPILLARY FORCES BETWEEN FLOATING PARTICLES" in Particles at Fluid I nterfaces and Membranes: Attachment of Colloid Particles and Proteins to Interfaces and formation of two-dimensional arrays. *Elsevie r, Amsterdam* (2000).
59. J. Yuan, J. Feng, S. K. Cho, Dielectrowetting control of capillary force (Cheerios effect) between floating objects and wall for dielectri c fluid. *Micromachines* **12**, 341 (2021).
60. J. Li, B. D. Favis, Characterizing co-continuous high density polyethylene/polystyrene blends. *Polymer* **42**, 5047-5053 (2001).
61. D. Y. Kwok *et al.*, Low-rate dynamic contact angles on polystyrene and the determination of solid surface tensions. *Polym. Eng. Sci.* **3 8**, 1675-1684 (1998).
62. N. De Geyter, R. Morent, C. Leys, Surface characterization of plasma-modified polyethylene by contact angle experiments and ATR-F TIR spectroscopy. *Surf. Interface Anal.* **40**, 608-611 (2008).
63. S. R. Holmes-Farley, C. D. Bain, G. M. Whitesides, Wetting of functionalized polyethylene film having ionizable organic acids and ba ses at the polymer-water interface: Relations between functional group polarity, extent of ionization, and contact angle with water. *Lan gmuir* **4**, 921-937 (1988).
64. A. Zdziennicka, K. Szymczyk, J. Krawczyk, B. Jańczuk, Some remarks on the solid surface tension determination from contact angle measurements. *Appl. Surf. Sci.* **405**, 88-101 (2017).
65. H. Schonherr, Z. Hruska, G. J. Vancso, Surface characterization of oxyfluorinated isotactic polypropylene films: Scanning force micro scopy with chemically modified probes and contact angle measurements. *Macromolecules* **31**, 3679-3685 (1998).
66. O. J. Kwon, S. Tang, S. W. Myung, N. Lu, H. S. Choi, Surface characteristics of polypropylene film treated by an atmospheric pressur e plasma. *Surf. Coat. Technol.* **192**, 1-10 (2005).